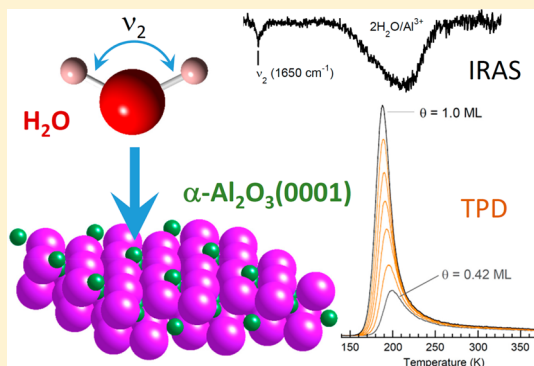


Molecular Water Adsorption and Reactions on α - $\text{Al}_2\text{O}_3(0001)$ and α -Alumina ParticlesNikolay G. Petrik,[†] Patricia L. Huestis,[‡] Jay A. LaVerne,[‡] Alexandr B. Aleksandrov,[§] Thomas M. Orlando,[§] and Greg A. Kimmel^{*,†,§}[†]Physical Sciences Division, Pacific Northwest National Laboratory, P.O. Box 999, Richland, Washington 99352, United States[‡]Radiation Laboratory and Department of Physics, University of Notre Dame, Notre Dame, Indiana 46556 United States[§]School of Chemistry and Biochemistry, Georgia Institute of Technology, Atlanta, Georgia 30332, United States

ABSTRACT: The adsorption and reaction of water on single crystal α - $\text{Al}_2\text{O}_3(0001)$ in ultrahigh vacuum, and α -alumina particles in ambient conditions, were investigated using temperature-programmed desorption (TPD), infrared reflection absorption spectroscopy (IRAS), diffuse reflectance infrared Fourier transform spectra (DRIFTS), and other surface science techniques. For a water coverage of $1 \text{ H}_2\text{O}/(\text{surface Al}^{3+})$ on α - $\text{Al}_2\text{O}_3(0001)$, no evidence for the surface hydroxyls expected from dissociative adsorption was observed in the infrared spectra, while the ν_2 vibration of molecular water was observed. Electron-stimulated desorption of molecular water at low coverages also indicated molecular or mixed (molecular plus dissociative) adsorption. Analysis of Kr TPD spectra showed that the water films wet the alumina substrate and suggested that the films were initially growing layer-by-layer. In contrast with the single crystal results, DRIFTS of water adsorption on alumina particles indicated the presence of surface hydroxyls that persist even after annealing to high temperatures in oxygen. For water on α - $\text{Al}_2\text{O}_3(0001)$ at coverages less than $0.3 \text{ H}_2\text{O}/(\text{surface Al}^{3+})$, water desorbed over a broad temperature range extending from ~ 250 to 700 K . For larger coverages, water desorption occurred at temperatures between ~ 160 and 250 K , consistent with desorption of molecular water. The results, which are consistent with at most a small amount of water dissociation on the Al-terminated (0001) surface, are difficult to reconcile with calculations suggesting that the barrier to dissociation is small. However, the results are consistent with recent vibrational sum frequency experiments showing that the hydroxylation of the Al-terminated (0001) surface takes many days even at ambient pressures and temperatures.



I. INTRODUCTION

Alumina and its interactions with water are important in areas ranging from electronics and catalysis to environmental science,^{1–4} and as a result, it has been extensively studied.^{5–23} For α -alumina in ultrahigh vacuum (UHV) conditions, experiments^{24,25} and theory^{7,14} show that the (0001) surface is Al-terminated. In this configuration, the topmost layer is a hexagonal array of aluminum atoms, which have an areal density of $5.00 \times 10^{18} \text{ m}^{-2}$. These aluminum atoms, Al_s , are relaxed compared to their bulk positions such that they are nearly coplanar with the first layer of oxygen atoms, O_s . The interlayer spacing between the first layers of aluminum and oxygen is predicted to be ~ 0.01 – 0.02 nm .^{7,14,26} The oxygen atoms are also arranged in a hexagonal array with an areal density that is 3 times larger than the Al_s . Density functional theory (DFT) calculations predict that molecular water binds to Al_s through the oxygen lone-pair electrons and adsorbs nearly parallel to the surface.^{7,14,17} However, the calculations show that molecular adsorption is metastable with respect to dissociative adsorption by ~ 0.3 – 0.4 eV .^{7,15,27} Dissociation creates two hydroxyl groups on the surface: One hydroxyl, OH_{ad} , contains the oxygen from the water molecule and is

bound on top of an Al_s . The second hydroxyl, OH_{surf} , results from the hydrogen atom transferred to a substrate oxygen atom. The stability of the dissociated state relative to the molecular state depends on which surface oxygen atom accepts the hydrogen atom from the water molecule.^{7,15,17,21,27} The dissociation can be characterized as heterolytic, such that the two species formed are $\text{Al}_s\text{--OH}^-$ ($\equiv \text{OH}_{\text{ad}}$) and $\text{O}_s\text{--H}^+$ ($\equiv \text{OH}_{\text{surf}}$).^{15,16} The barrier for dissociation is expected to be modest ($\sim 0.2 \text{ eV}$)^{15,17,27} such that the lifetime of the molecular state should be less than 10^{-10} s (10^{-8} s) at 300 K (100 K).¹⁷ Several different vibrational frequencies have been proposed for the O–H stretch for the hydroxyl groups.^{7,17,27} For OH_{ad} , the frequency is predicted to be $\sim 3780 \text{ cm}^{-1}$.^{15,27} The calculated frequency for OH_{surf} is significantly red-shifted (~ 3430 – 3560 cm^{-1}), perhaps putting it in the range of the O–H stretching band of water. However, vibrational sum-frequency generation (vSFG) measurements found that both types of hydroxyls are blue-shifted with respect to the O–H stretch band of water.¹⁹

Received: February 26, 2018

Revised: April 11, 2018

Published: April 19, 2018



Both types of hydroxyls also have components of their O–H stretch vibrations that are normal to the surface.^{15,19,20} Schneider and co-workers investigated water adsorption at a coverage, θ , of $1.0 \times 10^{19} \text{ m}^{-2}$. At this coverage, all the water molecules (either dissociated or molecular) form a bond with the alumina substrate, while at higher coverages the additional water is not expected to interact directly with the substrate. Thus, we will define 1 monolayer (ML) to be $1.0 \times 10^{19} \text{ m}^{-2}$. Note that this 1 ML coverage is quite close to the surface density of water molecules in the basal plane of hexagonal ice, which $1.14 \times 10^{19} \text{ m}^{-2}$ at 145 K.²⁸

A variety of experimental techniques have been used to investigate the adsorption and reactions of water on $\alpha\text{-Al}_2\text{O}_3(0001)$. Using temperature-programmed desorption (TPD) and laser-induced thermal desorption, George and co-workers proposed that water dissociatively adsorbs at 300 K with an initial sticking coefficient of ~ 0.1 .^{8,29} Hydroxyl coverages as large as 0.5 ML were reported, but only after water exposures of $\sim 10^{10}$ langmuirs (where 1 langmuir = 10^{-6} Torr-s). The water vapor pressure during dosing was 0.25 Torr for those experiments. X-ray photoelectron spectroscopy (XPS) experiments of water adsorption on $\alpha\text{-Al}_2\text{O}_3(0001)$ also found significant hydroxylation after water exposures of more than 10^9 langmuirs (180 s at 10 Torr) at 300 K.⁹ Dehydroxylation was observed during the XPS measurements, possibly accounting for the apparent lack of reactions at lower water exposures (e.g., 10^6 langmuirs) where the TPD experiments observed dissociation. In contrast, a peak at 3720 cm^{-1} , attributed to hydroxyls, was observed in high-resolution electron energy loss spectroscopy (HREELS) after water exposures of only 450 langmuirs (600 s at 7.5×10^{-7} Torr) at room temperature.⁵ The reasons for the differences in the amount of water exposure required to hydroxylate the surface, or even the structure of the “hydroxylated surface”, in these various experiments are unclear. But differences in surface preparation techniques and other experimental details are plausible candidates.

The equilibrium structure of the (0001) surface of α -alumina at ambient conditions is quite different than the Al-terminated surface found in a vacuum.^{10,11,21} X-ray scattering measurements show that the surface is oxygen terminated with a structure that is similar to gibbsite ($\text{Al}(\text{OH})_3$); i.e. it is fully hydroxylated.¹⁰ This observation agrees with theoretical predictions that the aluminum termination has a lower surface energy for bare surfaces, while the oxygen termination is lower for hydroxylated surfaces.³⁰ The pathways by which an Al-terminated surface can be converted to a hydroxylated, O-terminated surface have been investigated with DFT.^{15,17} These studies concluded that water dissociation on the Al-terminated surface, as outlined above, produced a surface that was not readily converted to the fully hydroxylated, oxygen-terminated surface. Recent vSFG measurements support this picture.²⁰ In those experiments, an Al-terminated $\alpha\text{-Al}_2\text{O}_3(0001)$ single crystal was prepared in UHV by sputtering and annealing. The crystal was then removed into air and the surface was monitored via vSFG. Surprisingly, it took many days for the surface hydroxyls to appear in the spectra. Note that the water vapor pressure in the laboratory was estimated at 8.5 Torr, such that each day corresponded to an exposure of $\sim 7 \times 10^{11}$ langmuirs.

Here we investigate the adsorption and reactions of water on $\alpha\text{-Al}_2\text{O}_3(0001)$ in UHV using TPD, infrared reflection absorption spectroscopy (IRAS), electron-stimulated desorption (ESD), and other surface science techniques. The results

on the single crystal alumina surface are compared to similar experiments on α -alumina particles in ambient conditions. Diffuse reflectance infrared Fourier transform spectroscopy (DRIFTS) shows that calcining α -alumina particles in air produces surfaces that readily react with water to form at least four different hydroxyl species. Molecular water adsorbs on these hydroxylated particles at room temperature and desorbs at $\sim 405 \text{ K}$. Recombinative desorption continues to $T > 700 \text{ K}$. In contrast, IRAS for $\theta = 0.5 \text{ ML}$ on $\alpha\text{-Al}_2\text{O}_3(0001)$ did not show any evidence of the hydroxyls expected from dissociated water, but the ν_2 mode for molecular water was observed, indicating molecular adsorption. Measurements of ESD yield of molecular water versus water coverage, which increased approximately linearly with coverage for $0 \leq \theta < 2 \text{ ML}$, also suggest that water adsorbs in the molecular state, or perhaps a mixture of molecular and dissociated states, in this coverage range. For $\theta < 0.15 \text{ ML}$ on $\alpha\text{-Al}_2\text{O}_3(0001)$, water desorbed over a wide range of temperatures ($\sim 250\text{--}700 \text{ K}$). For coverages between 0.15 and 1 ML, the water desorbed in much narrower temperature range around 200 K. Desorbing the water films by heating to 950 K produced a hydroxyl-free, Al-terminated surface, showing that any dissociative adsorption was reversible. Kr desorption from the water-covered surfaces indicates the water layers adsorbed at 100 K grow layer-by-layer for at least the first 2 ML. The current results are compared to previous IR measurements of water adsorbed on $\alpha\text{-Al}_2\text{O}_3(0001)$ at room temperature and relative humidities of $\sim 1\%$ and on hydroxylated α -alumina particles.

II. EXPERIMENT

The experiments were performed using techniques that have been described previously.^{23,31} The experiments on single-crystal, $\alpha\text{-Al}_2\text{O}_3(0001)$ were performed in an UHV system with a base pressure of $\sim 7 \times 10^{-11}$ Torr. That system includes a closed-cycle He cryostat for cooling the sample, a molecular beam dosing system, a quadrupole mass spectrometer (Extrel), a Fourier transform infrared spectrometer (Bruker, Vertex 80) set up in external reflection mode for IRAS, and a low-energy electron gun (Kimball Physics, ELG-2). The $10 \times 10 \times 0.1 \text{ mm}^3$, $\alpha\text{-Al}_2\text{O}_3(0001)$ ($<0.5^\circ$) single crystal (Princeton Scientific) was mounted on a tantalum base plate using ceramic adhesive (Aremco) and a retaining ring. The sample temperature was controlled by resistively heating the base plate. The temperature was monitored by a K-type thermocouple spot-welded to the base plate. The temperature of the alumina surface was calibrated by measuring the desorption rate from a multilayer crystalline ice film and using the known vapor pressure of crystalline ice. The base temperature for the sample was $\sim 40 \text{ K}$. (The base temperature for a newly mounted sample is typically $\sim 25 \text{ K}$, and this slowly increases over time as the number of heating and cooling cycles for the sample increases.) The sample was initially cleaned by multiple cycles of sputtering with 2 keV Ne^+ and annealing at 1050 K for 2 min (typical). This procedure for preparing the sample has been shown to produce an ordered surface with a 1×1 LEED pattern.^{19,20} After initially cleaning the sample, we found that for subsequent sputtering and annealing cycles, annealing with and without O_2 exposure led to very similar results.

Water and other gases were dosed on the $\text{Al}_2\text{O}_3(0001)$ substrate using an effusive molecular beam source. For water dosing, the molecular beam flux is known based on our previous research investigating the structure of water adlayers on Pt(111) and rutile $\text{TiO}_2(110)$.^{32–34} For the water

adsorption temperatures ($100\text{ K} \leq T \leq 140\text{ K}$) and coverages in the experiments presented here, we have verified that the water condensation coefficient is ~ 1 and independent of coverage. Therefore, the absolute water coverage is determined from the dosing time. The relative coverage (in monolayers) is then determined using the monolayer definition ($1\text{ ML} \equiv 1.0 \times 10^{19}\text{ m}^{-2}$). The diameter of the molecular beam at the sample was 7 mm for the umbra (7.6 mm for the penumbra). For the electron-stimulated desorption measurements, the electron beam was incident at 40° from the surface normal. The irradiations were performed with 100 eV electrons. A focused electron beam, which had a diameter of $\sim 1.5\text{ mm}$, was rastered over the surface to provide a uniform irradiation.³⁵ The instantaneous current density in the beam was $1.8 \times 10^{15}\text{ e}^-/\text{cm}^2/\text{s}$, and the fluence for a single scan (0.4 s duration) over the surface was $1.5 \times 10^{13}\text{ e}^-/\text{cm}^2$.

The infrared s- and p-polarized light was incident on the $\text{Al}_2\text{O}_3(0001)$ single crystals at grazing incidence ($\sim 85^\circ$ with respect to normal) and detected in the specular direction. For s-polarized light, the electric field vector is parallel to surface, and therefore those spectra are sensitive to vibrations that have transition dipole moments parallel to the surface. Note that on dielectric substrates for s-polarized light the absorbance, $A = \log(R_0/R)$, is always negative due to optical effects.^{36,37} For p-polarized light, the electric field vector has components perpendicular and parallel to the surface. For the geometry used in the current experiments, modes that are perpendicular to the surface show up as negative absorbance ("emission") peaks, while modes that are parallel to the surface show up as positive peaks.^{32,36} No appreciable differences were found between IR spectra measured with the IR beam incident along both the $[11\bar{2}0]$ and the $[1\bar{1}00]$ azimuths. The averaged spectra shown below have used results from both azimuths. Because the IRAS signals from films that are only few monolayers thick on dielectric substrates are so weak, the spectra reported below were all averages of many individual experiments. For a typical set of experiments, the sample was cleaned either by sputtering and annealing in oxygen or simply annealing in oxygen prior to starting. (The results are the same in either case.) Each individual experiment then consists of the following sequence: (1) The sample is briefly heated to 950 K to desorb any adsorbates from the surface. (2) A reference spectrum, R_0 , is obtained from the clean sample with $T < 70\text{ K}$. (3) Water is deposited at the desired temperature (140 K for most of the spectra shown below). (4) A reflectance spectrum for the adsorbed film, R , is obtained at $T < 70\text{ K}$, typically with 3000 scans of the interferometer. This sequence is then repeated until the desired signal-to-noise ratio is achieved. Because of the small signals and slow changes in the system ("drift"), it is important to have reference spectra taken relatively close in time to the reflectance spectra for the adsorbed layers of interest. Therefore, we have found that more individual experiments with fewer scans per experiment produce better results than fewer individual experiments with more scans per experiment. Most of the spectra shown below are the average of anywhere from 8 to 40 individual experiments. (The system is computer controlled, and many of the experiments are run overnight.) The resolution for the spectrometer was set to 4 cm^{-1} . However, as will be seen below, all of the absorbance features that were detected for water adsorbed on $\text{Al}_2\text{O}_3(0001)$ are considerably broader than 4 cm^{-1} . As a result, none of the IR spectra are affected by the instrumental resolution. In addition, the frequencies mentioned in the discussion of various

features in the IR spectra are meant to facilitate the discussion and are not meant to imply any spectral resolution beyond what is apparent in the spectra.

Aluminum oxide powder (α -phase, Alfa Aesar, 99.95%) was baked in air at 773 K to remove organic impurities. Powders were then exposed to water vapor in 53% relative humidity chambers for several days and allowed to equilibrate. Diffuse reflectance infrared Fourier transform spectroscopy (DRIFTS) was performed using a Bruker Vortex 70 with a Harrick Praying Mantis high temperature cell. The background spectrum was taken of pure KBr. The TPD measurements were performed on sample masses of approximately 100 mg that were deposited into a custom cell containing a cartridge heater. The cell was heated from 298 to 773 K at a rate of 5 K/min while the desorbing gases were monitored using a Pfeiffer Prisma quadrupole mass spectrometer. Water was found to be the main gaseous component and was monitored at a mass to charge ratio of 18. The background measurement was done on an empty cell before each run and was subtracted from the sample spectrum.

III. RESULTS AND DISCUSSION

Figure 1 shows a series of D_2O temperature-programmed desorption (TPD) spectra for coverages ranging from 0.026 to

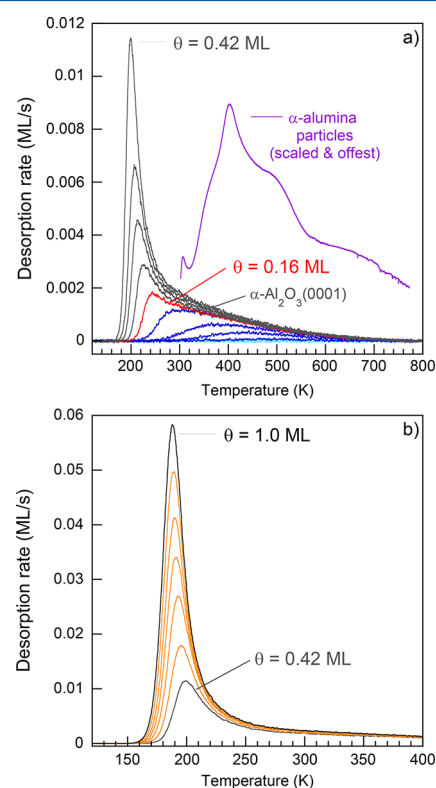


Figure 1. TPD spectra of D_2O adsorbed on $\alpha\text{-Al}_2\text{O}_3(0001)$ at 100 K and H_2O on α -alumina particles at room temperature. The heating rate was 2 K/s. (a) Spectra for D_2O coverages, θ , from 0 to 0.42 ML, where 1 ML is defined as 1×10^{19} molecules/ m^2 . For $\theta < 0.16\text{ ML}$ (a, red line), the water desorbs from the single-crystal surface over a broad range of temperatures that might indicate recombination and desorption of dissociated water. However, water desorption from the (0001) surface is quite different than desorption from α -alumina particles (purple line). (b) Spectra for $0.42\text{ ML} \leq \theta \leq 1.0\text{ ML}$. At higher coverages, the water desorbs over a relatively narrow temperature range typical for molecular adsorption.

1 ML on α -Al₂O₃(0001) for D₂O deposited at 100 K. Similar results were obtained for H₂O (data not shown). However, in that case, the background signal at 18 amu was somewhat higher. Measurements of the partial pressure of water during deposition of the water films and the integrated D₂O TPD signal versus D₂O dose show that the condensation coefficient is large (~ 1) and nearly independent of coverage, as expected at 100 K.^{38,39} These characteristics facilitate accurate determination of the water coverage. For the lowest coverages (e.g., $\theta < 0.16$ ML), the water desorbs over a broad range of temperature from ~ 250 to 700 K (Figure 1a). As the coverage increases, the onset temperature for desorption decreases, while the desorption rate at higher temperatures is nearly independent of coverage. TPD spectra similar to those shown in Figure 1a for water on α -Al₂O₃(0001) have been reported previously.^{8,19,29} Figure 1a also shows the TPD spectrum for water adsorbed on α -alumina particles at room temperature (purple line). For these particles, which were prepared by heating in air at 773 K, the TPD spectrum has a peak at ~ 405 K and a shoulder at ~ 500 K. For water on many surfaces, such high desorption temperatures are associated with the recombination and desorption of dissociatively adsorbed water,⁴⁰ and desorption at high temperatures is often taken as evidence of recombinative desorption. However, DRIFTS data discussed below indicate that desorption of molecular water contributes to the TPD peak at ~ 405 K on the alumina particles, while desorption at $T > 400$ K is associated with recombinative desorption. For coverages between ~ 0.42 and 1.0 ML on α -Al₂O₃(0001), most of the D₂O desorbs over a relatively narrow temperature range (Figure 1b). However, the leading edges of the TPD spectra continue to move to lower temperatures while the high-temperature edges are still coaligned. These spectra indicate that the free energy of the water layer increases (i.e., it becomes less stable) as the coverage increases α -Al₂O₃(0001). Water desorption in this temperature range is typically associated with molecular water.⁴⁰ For coverages greater than 3 ML, the leading edges of the TPD spectra are coaligned, indicating that the free energy of the water film is no longer changing as the coverage increases (data not shown).

Insight into the structure of the water layer adsorbed on α -Al₂O₃(0001) can be gained by measuring the amount of water needed to completely “cover” the surface (i.e., block all the adsorption sites). Previous research has shown that the adsorption and desorption of rare gases, or other weakly interacting adsorbates, can be used to assess how a water adlayer covers the substrate.^{33,34} The basic idea is that a rare gas binds more strongly to most substrates than to a water adlayer. Therefore, if portions of the substrate are exposed, the rare gas will preferentially adsorb there. Once the substrate is covered by the water adlayer all these higher energy binding sites will be gone, and this will be reflected in the TPD spectra. Figure 2a shows a series of Kr TPD spectra for various coverages of Kr deposited on the bare Al₂O₃(0001) at 40 K. The Kr TPD spectra display a single peak at 51 K that saturates for sufficiently large Kr doses (Figure 2a, green lines). This peak in the TPD spectra is associated with desorption from the Kr monolayer on Al₂O₃(0001). For small Kr coverages (Figure 2, red lines), the Kr desorbs at somewhat higher temperatures, perhaps due to surface defects such as step edges. At higher exposures, the monolayer peak saturates, but only a small shoulder grows in at lower temperatures suggesting that one monolayer of Kr readily adsorbs on Al₂O₃(0001) at 40 K, but

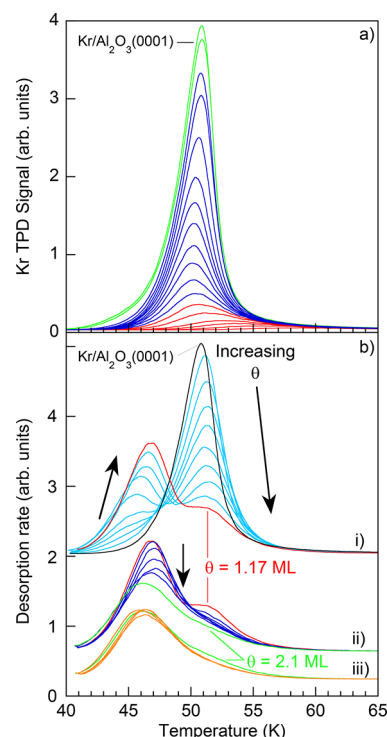


Figure 2. (a) Kr TPD spectra on α -Al₂O₃(0001) for several coverages of Kr. Kr adsorbed directly on the (0001) surface desorbs at ~ 51 K (blue lines). For small Kr coverages (red lines), the spectra extend to higher temperatures, probably due to interactions with defects on the surface such as step edges. For larger Kr doses, the alumina surface is covered and a small amount of additional Kr desorbs at lower temperatures (green lines), corresponding to a small amount of Kr in the second layer. (b) One monolayer Kr TPD spectra for several water coverages on α -Al₂O₃(0001). The water films were preadsorbed at 120 K, and then the sample was dosed with Kr at $T < 40$ K. (i) As the water coverages increase from 0 to ~ 1.1 ML, the amount of Kr desorbing at 51 K decreases and desorption at ~ 46 K, which corresponds to Kr desorbing from one layer of water, increases. (ii) For $1.1 \text{ ML} \leq \theta \leq 2.1 \text{ ML}$, the Kr desorption peak at ~ 46 K decreases. (iii) For $\theta > 2.1 \text{ ML}$, the Kr TPD spectra are largely independent of the water coverage.

not multilayers. This observation is also consistent with measurements of the Kr partial pressure during dosing which show a decrease in the Kr condensation coefficient once the substrate is covered with a layer of Kr (data not shown).

Figure 2b shows a series of Kr TPDs versus the amount of water preadsorbed on the surface. For this experiment, the water was adsorbed at 120 K, and then the sample was exposed to a saturation coverage of Kr at 40 K prior to obtaining the Kr TPD. For this experiment, the area of the Kr desorption peak at 51 K is approximately proportional to the fraction of the surface that is not covered by water.^{33,34} As the water coverage increases, the Kr TPD peak at 51 K decreases and a new, lower temperature peak develops at ~ 46 – 47 K. This lower temperature desorption is due to Kr desorbing from the water monolayer. Figure 3 shows the integrated intensity for Kr desorption from the bare surface (black circles) and one layer of water (red triangles) versus water coverage. For water coverages less than ~ 1.1 ML, the integrated intensity for the Kr desorbing from the bare surface decreases linearly, while Kr signal from one layer of water signal increases. At $\theta \sim 1.1$ ML, the integrated TPD signal for Kr desorbing from one layer of water reaches a maximum and then decreases as the higher

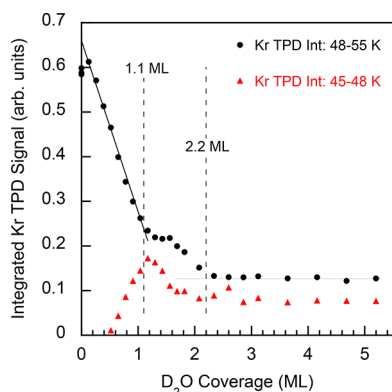


Figure 3. Integrated Kr TPDs versus D_2O coverage. Integrals over the peaks in the Kr TPD spectra shown in Figure 2 provide information on the growth of the water films on $\alpha-Al_2O_3(0001)$. Kr desorbing from the bare alumina surface (black circles) decreases linearly up to a water coverage of ~ 1.1 ML, at which point the integral for Kr desorbing from one layer of water (red triangles) reaches a maximum, and then decreases until $\theta > 2.1$ ML, at which point the Kr TPD no longer change with increasing water coverage.

coverages as the second layer forms. The Kr TPD data indicate that the first water layer wets the $Al_2O_3(0001)$ surface and has an areal density that is comparable to that of a water layer in hexagonal ice ($1.14 \times 10^{19} \text{ m}^{-2}$).²⁸ The data also suggest that the second layer wets the first (i.e., the water films grow layer-by-layer on the alumina). Note that DFT calculations for two different structures of the water monolayer on $Al_2O_3(0001)$ —one for molecularly adsorbed water and a second with a mixed dissociated and molecularly adsorbed layer—have densities of 1.0 ML.¹⁵ Either of these calculated water layer structures would be consistent with the Kr TPD results in Figures 2 and 3.

A key question concerning water's interaction with $Al_2O_3(0001)$ is whether the water dissociates on the surface, remains intact, or forms a mixed molecular-dissociated layer. The reaction pathway and kinetics of dissociation are also an open question.^{15,20,21} We have used two different approaches to assess the adsorption configuration in the water adlayer: infrared reflection absorption spectroscopy (IRAS) and electron-stimulated desorption (ESD). ESD experiments can be useful because irradiating adsorbed water films with low-energy electrons (e.g., 100 eV) produces electronic excitations within the films that can lead to prompt, nonthermal desorption of molecular water (along with a number of other nonthermal reactions).^{41–43} Thus, water ESD provides information on molecular versus dissociative adsorption because different reaction pathways are required to recombine and desorb dissociated water versus the direct ejection of molecularly adsorbed water after electronic excitation. The infrared spectra of water adsorbed on surfaces can also provide valuable insight into the state of the adsorbed water (i.e., molecular versus dissociative adsorption) and the bonding geometry within the water layer.^{32,44–48} For example, water dissociation leading to the formation of surface hydroxyls often produces relatively narrow IR peaks that are blue-shifted relative to the broad OH-stretch band associated with hydrogen-bonded water.^{48–50}

The integrated D_2O ESD versus the D_2O coverage (circles) is shown in Figure 4. The D_2O was deposited at 130 K and irradiated with 100 eV electrons at 100 K. For $\theta \leq 1$ ML, the D_2O ESD signal increases approximately linearly. The dashed line shows a linear fit to the data for this coverage range. For 1

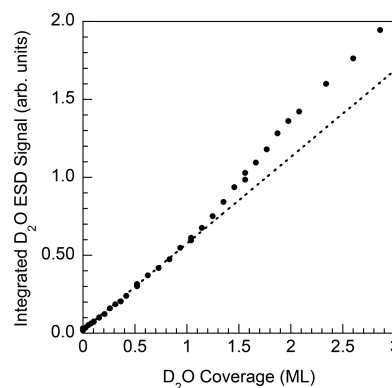


Figure 4. Integrated D_2O electron-stimulated desorption vs D_2O coverage on $\alpha-Al_2O_3(0001)$. The linear increase in the D_2O ESD signal shows that molecular water is present even at the lowest coverages on this surface.

ML $< \theta < 3$ ML, the D_2O ESD yield continues to increase, but at a slightly greater rate (Figure 3). The initial linear increase in the D_2O ESD indicates that molecular water is adsorbed on the surface even at the lowest coverages on $Al_2O_3(0001)$. While the ESD results do not rule out the possibility of mixed (i.e., molecular and dissociative) adsorption, the linear increase might indicate that the fraction of molecular versus dissociative adsorption is not changing for $0 < \theta \leq 1$ ML.

Figure 5 shows the s- and p-polarized IRAS spectra for both H_2O and D_2O for $\theta = 0.5$ ML. Recall that at this coverage there is one water molecule per surface Al^{3+} . For these experiments,

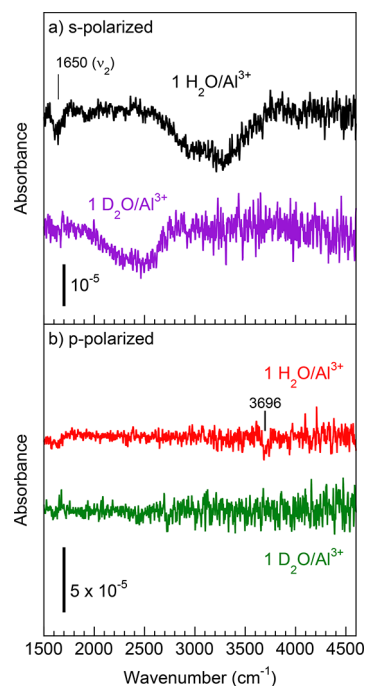


Figure 5. Infrared reflection absorption spectra (IRAS) for H_2O and D_2O adsorbed on $\alpha-Al_2O_3(0001)$ for $\theta = 0.5$ ML, which corresponds to one water molecule for each aluminum ion on the surface. (a) Bands associated with the OH- and OD-stretch of molecular water and/or hydroxyls are observed with s-polarized light. In addition, the ν_2 mode of molecular water is evident for H_2O . (b) With p-polarized light, the signals are small, but a small peak is discernible at 3696 cm^{-1} for H_2O .

the water was deposited at 140 K, and the IR spectra were obtained at $T < 70$ K. With s-polarized light, both H₂O and D₂O have weak, broad absorbances in the OH- and OD-stretch regions that are characteristic of hydrogen-bonded water layers (Figure 5a, black and purple lines, respectively). For H₂O, the ν_2 mode for molecular water is also observed at 1650 cm⁻¹. For D₂O, the ν_2 mode is at a frequency where artifacts in the IR spectra make it difficult to observe such small signals. With p-polarized light, no IR signal was observed above the noise for D₂O (Figure 5b, green line). However, a small negative peak at ~ 3696 cm⁻¹ is just discernible for H₂O (Figure 5b, red line). Compared to bulk water, the OH- and OD-stretch bands on Al₂O₃(0001) observed with s-polarized light extend to considerably lower frequencies: The OH-stretch band, measured at 10% of the maximum adsorbance, extends from ~ 2650 to 3710 cm⁻¹ on Al₂O₃(0001), while the corresponding range for bulk water is only from ~ 3000 to 3500 cm⁻¹.^{51,52} Because the measured frequencies for the surface hydroxyls on α -Al₂O₃(0001) are all blue-shifted relative to the OH-stretch band of bulk water,¹⁹ the low-frequency portions of the spectra in Figure 6 are probably not due to dissociative adsorption. For

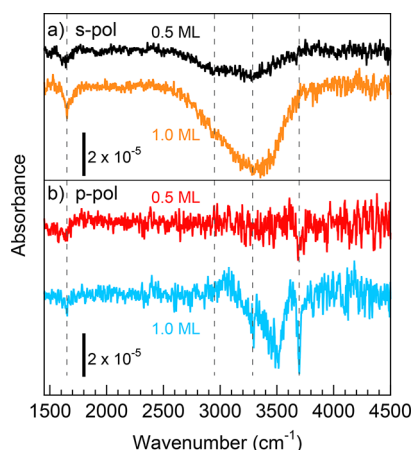


Figure 6. IRAS for H₂O adsorbed on α -Al₂O₃(0001) for $\theta = 0.5$ and 1.0 ML. (a) For s-polarized, the ν_2 mode for molecular water is observed for both coverages. However, the integrated intensity in the OH-stretch region at 1 ML (orange line) is approximately 3 times larger than the intensity at 0.5 ML (black line), and the extra intensity is predominantly at higher frequencies. (b) For p-polarized light at $\theta = 1$ ML (blue line), negative peaks—corresponding to vibrations normal to the surface—are found at 3285, 3500, and 3696 cm⁻¹.

a wide variety of hydrogen-bonded minerals, the frequency of the OH-stretch is correlated to the oxygen–oxygen (O–O) distance for the bond.⁵³ If we assume a similar correlation holds for water adsorbed on a surface, then the broad IR spectra would correspond to a broad range of O–O distances within the water adlayer.⁵⁴ However, given that other hydrogen-bonded species (such as Zundel or Eigen complexes) can also produce low-frequency vibrations,^{55,56} comparisons with the calculated vibrational dynamics for various water adlayers on Al₂O₃(0001) are needed to better understand these spectra.

For $\theta = 1$ ML, the s-polarized absorbance is approximately 3 times larger than the signal at half that coverage (Figure 6a). While the OH-stretch band extends over the same broad range at $\theta = 0.5$ and 1 ML, most of the additional intensity in the IRAS signal at 1 ML is at higher frequencies, suggesting the additional water is more weakly bound (in agreement with the changes in the TPD from 0.5 to 1.0 ML; see Figure 1). The ν_2

mode for molecular water is observed at 1650 cm⁻¹ for both $\theta = 0.5$ and 1.0 ML. With p-polarized light (Figure 6b), the signal at $\theta = 1$ ML is considerably stronger than at half that coverage. A narrow peak at 3696 cm⁻¹, which was barely visible at the lower coverage, is now clearly seen. In addition, a broad absorbance with a (negative) peak at ~ 3500 cm⁻¹ is apparent. Another peak, which approximately matches the position of the absorbance seen with s-polarized light, appears at 3290 cm⁻¹.

The absorbance peak at 3696 cm⁻¹ for $\theta = 1$ ML corresponds very closely with the frequency of the dangling OH peak observed on the surface of multilayer ASW or crystalline ice films.^{57,58} Figure 7 shows an expanded view of

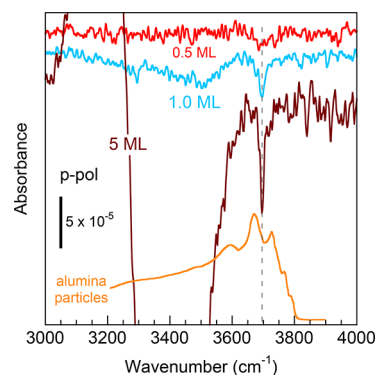


Figure 7. The p-polarized IRAS for H₂O adsorbed on α -Al₂O₃(0001) and the IR spectrum for hydroxylated α -alumina particles.⁴⁹ The peak at 3696 cm⁻¹ for $\theta = 1$ ML (blue line) matches the dangling OH peak of molecular that is observed at the vacuum interface of multilayer water films (e.g., $\theta = 5$ ML, brown line).⁵⁷ The dangling OH peak for molecular water does not match surface hydroxyl peaks observed on α -alumina particles (orange line: the reported signal was scaled to facilitate comparison with the IRAS data).

the dangling OH-stretch region of the p-polarized spectra for $\theta = 0.5$, 1.0, and 5 ML on α -Al₂O₃(0001). The 5 ML water film was deposited at 100 K, and the displayed spectrum is the average of only 10⁴ scans (versus $\sim 10^5$ scans for 0.5 and 1.0 ML). Despite the higher noise level in the 5 ML spectrum, the dangling OH peak is easily observed. The integrated intensity of the dangling OH peak is about 3 times larger for the 5 ML water film compared to the 1 ML film and more than 10 times larger than the 0.5 ML water film. Note that the magnitude of the dangling OH peak is approximately independent of the water coverage for $\theta \geq 5$ ML (data not shown). This observation is expected for nonporous films that are sufficiently thick that the structure of the water/vacuum interface is independent of the water/substrate interface. The coverage of these dangling OH groups, θ_{dOH} , on the surface of ASW is not known in detail, but probably one-quarter or fewer of the molecules on the surface have a dangling OH (i.e., $\theta_{\text{dOH}} < 0.25$ ML for ASW). Thus, it is likely that less than 10% of the water present in the film at $\theta = 1$ have dangling OH groups. At $\theta = 0.5$ ML, the amount of dangling OH's is considerably less ($\theta_{\text{dOH}} \lesssim 0.03$ ML).

We have also investigated the adsorption of water on α -Al₂O₃(0001) at 300 K. For water exposures at that temperature where the sample is allowed to cool to its base temperature after dosing the water, the resulting water coverage is less than 0.15 ML. In that case, we did not observe any signal in IRAS (at comparable signal-to-noise levels to the data shown in Figures 5 and 6) for either s- or p-polarized light (data not shown). The

lack of a peak corresponding to surface hydroxyls for p-polarized light can be compared to previous IRAS measurements on hydroxylated $\text{TiO}_2(110)$ where the coverage of “bridging hydroxyls” was ~ 0.1 ML (with the ML definition used here).⁵⁹ On a hydroxylated surface without any coadsorbed molecular water, these non-hydrogen-bonded hydroxyls produce a narrow peak at 3711 cm^{-1} in p-polarized IRAS. The magnitude of the absorbance for the bridging hydroxyls, $\sim 2 \times 10^{-4}$, is large enough that non-hydrogen-bonded hydroxyls with a comparable oscillator strength and at comparable coverages should be observable in IRAS on $\alpha\text{-Al}_2\text{O}_3(0001)$. The absence of a comparable signal for water adsorbed at 300 K suggests that the resulting water adlayer on alumina is either purely molecular or mixed adsorption in those conditions.

For p-polarized light, the electric field has components perpendicular and parallel to the surface and these two components contribute to the reflectance in different ways: A molecule with a transition dipole moment for a mode that is purely parallel to the surface will have a *positive* peak in the p-polarized IRAS, while a mode that is perpendicular to the surface will have a negative peak.^{36,37} For a vibrational mode that is inclined with respect to surface normal, these two components will counteract each other, resulting in a smaller signal. With s-polarized light, the electric field is parallel to the surface and only components of the vibrational modes that are parallel to the surface are detected. These modes always show up as negative absorbances, and there is no cancellation effect. These aspects of IRAS from dielectric substrates give us some important insight into the structure of the water films on $\text{Al}_2\text{O}_3(0001)$ at low coverages. For example, the dangling OH peak observed as a negative peak at 3696 cm^{-1} in the p-polarized spectra is not seen in the s-polarized spectra for $\theta = 1$ ML (see Figure 6). This suggests these OH groups are oriented normal, or nearly normal, to the surface. (However, for $\theta = 0.5$ ML, the signal is weak enough that we cannot say much about the orientation of the dangling OHs.) For $\theta = 0.5$ ML, a broad band of hydrogen-bonded water and/or hydroxyls is seen with s-polarized light, but not p-polarized light (see Figure 5). Note however that the lack of signal with the p-polarized light is not just a sensitivity issue: At $\theta = 1$ ML with p-polarized light, a broad, negative band is seen in addition to the narrow dangling OH peak at 3696 cm^{-1} (see Figure 6). Instead, the lack of a signal with p-polarized light for 0.5 ML indicates that the water molecules are oriented at an angle with respect to the surface normal such that the positive and negative components in the p-polarized signal have largely canceled each other. For larger water coverages, the net orientation of the molecules changes and the fortuitous cancellation observed at $\theta = 0.5$ ML is lifted.

As described in the Introduction, DFT calculations for 0.5 ML suggest that every water molecule should dissociate such that each Al_s has an OH_{ad} adsorbed on it.^{7,15–17,27} These non-hydrogen-bonded surface hydroxyls should have a significant component of their OH-stretch normal to the surface.^{15,19,20} In contrast, intact water molecules should adsorb on top of aluminum ions nearly parallel to the surface.¹⁵ However, the distance between Al_s sites is large enough that adsorbed water molecules would not form hydrogen bonds with their neighbors. Thus, for $\theta = 0.5$ ML, the IRAS results are not consistent with either purely dissociative adsorption or molecular adsorption at the Al_s sites. In addition, the calculations predict that the barrier to dissociation is only ~ 0.2 eV. With such a low barrier and assuming a normal

prefactor (e.g., $\nu = 10^{13}\text{ s}^{-1}$), a simple estimate of the lifetime of molecular water at 140 K (the temperature at the water was adsorbed) is $\sim 10^{-6}$ s. Such a short lifetime is consistent with more detailed calculations that also predict rapid dissociation for molecular water even at low temperatures.¹⁷ Therefore, the apparent lack of dissociated water at $\theta = 0.5$ ML should not be due to kinetic limitations. A plausible hypothesis to explain the observations is that the water adsorbs in a hydrogen-bonded islands (i.e., 2-dimensional clusters) at $\theta = 0.5$ ML, perhaps including some dissociated water, where the OH-stretch vibrations have components parallel and perpendicular to the surface. Island adsorption is consistent with the linear increase in the water ESD versus coverage (Figure 4). Because the adsorption of isolated water molecules is expected to block more of the substrate per molecule than adsorption in islands, island adsorption is also consistent with the Kr TPD experiments (Figures 2 and 3). At the adsorption temperatures used in the current experiments, the water molecules should be mobile on the surface, thus allowing for island formation. However, for adsorption at lower temperatures where the water mobility is limited, two-dimensional island formation should be inhibited.^{60,61}

Two-dimensional islands, where the local coverage within the island corresponds to 1 ML, could also be consistent with DFT calculations which indicate that the minimum-energy configuration at 1 ML is a 50–50 mixture dissociated and molecular water arranged in a flat, ice-like layer.^{15,16} For this adlayer structure, all the water molecules form four hydrogen bonds: three with neighboring OH_{ad} and one with an OH_s . In addition, all the surface hydroxyls also form hydrogen bonds. As a result, there should not be any dangling OH groups for this layer (i.e., consistent with the IRAS results). However, as the coverage increases above 0.5 ML, the IRAS and TPD results indicate that the additional water adsorbs molecularly so that by the time the surface is fully covered (i.e., $\theta = 1$ ML), most of the water is molecular. Therefore, the experimental results at 1 ML might correspond more closely to calculations for a water monolayer without any dissociation.¹⁵ That calculated structure, which is metastable with respect to the mixed monolayer, is also a flat, ice-like layer. In that case, half the water molecules bind to Al_s through one of the oxygen lone pair orbitals. The other half of the water molecules adsorb in an “H-down” configuration above 3-fold hollow sites on the surface^{15,62} or perhaps with a mixture of “H-down” and “H-up” water molecules.¹⁸ The dangling OH peak observed at 3696 cm^{-1} in the p-polarized signal at 1 ML is consistent with at least some water molecules adsorbed in an H-up configuration. Because vibrations associated with an “H-down” configuration are difficult to detect,⁶³ the lack of any signature for these species does not allow us to rule them out.

The ability to prepare a hydroxyl-free (0001) surface of alumina is debated in the literature. Several previous experiments have suggested that surface hydroxyls are difficult to remove from $\alpha\text{-Al}_2\text{O}_3(0001)$.^{6,24,64} However, other groups have reported procedures, such as sputtering and annealing the surface in UHV, that produce a hydroxyl-free, Al-terminated surface.^{19,20,29,65} For the IRAS results shown in Figures 5–7, the reference reflectance spectra, R_0 , were obtained from the $\alpha\text{-Al}_2\text{O}_3(0001)$ after briefly annealing to high temperature. (See the Experiment section for a detailed description of the procedures.) If the annealed surface contained hydroxyls, then the absorbance spectra obtained after adding water could be influenced by the presence of the hydroxyl bands in the

reference spectra and their loss upon the addition of a water adlayer. We conducted several control experiments to investigate this possibility and found no evidence for such an effect. One test involved preparing the alumina surface such that any remaining hydroxyls would be deuterated prior to obtaining R_0 . The surface was then exposed to H_2O to hydrogenate any hydroxyls on the surface before obtaining the reflectance spectra, R . In that case, the replacement of the OD bands in R_0 with the corresponding OH bands in R should result in a pair of bands with opposite signs in the absorbance spectra. However, the IRAS spectra were independent of whether the reference spectra were obtained from the deuterated or hydrogenated alumina surfaces. These results, which indicate that a hydroxyl-free, Al-terminated (0001) surface can be regenerated by heating in UHV, agree with Nelson et al., who reported that heating above 700 K in UHV desorbed all the water and eliminated any hydroxyls produced after exposing that surface to water at 300 K.²⁹

As discussed in the Introduction, the equilibrium surface terminations of alumina in vacuum, at ambient conditions, and in aqueous solutions are different. In wet or moist environments, the alumina surfaces should be hydroxylated.^{10,11,21} However, different experiments have led to quite different results regarding hydroxylation of the surfaces and the structure of the water layers in contact with these surfaces, particularly for the aqueous/(0001) interface.^{13,66,67} To compare the reactions of water with $\alpha\text{-Al}_2\text{O}_3$ (0001) in UHV with alumina surfaces in ambient conditions, we have measured the DRIFTS spectra for water adsorbed on α -alumina particles. For these experiments, alumina particles were first calcined in air at 773 K and then placed in a crucible at room temperature and 53% relative humidity where they were allowed to equilibrate over several days. The particles were then placed in a sealed IR cell, and the IR spectra were recorded at different temperatures. Figure 8 shows the spectra in the OH-stretch region obtained with the alumina particles heated to (a) 298, (b) 373, (c) 473, (d) 573, and (e) 673 K. At 298 K, the spectrum has a small peak at 3695 cm^{-1} characteristic of the dangling OH's observed on multilayer water films (see Figure 7), a broad absorbance extending from ~ 3000 to 3700 cm^{-1} due to hydrogen-bonded water adlayer, and a band at $\sim 1650\text{ cm}^{-1}$ associated with the ν_2 vibrations of molecular water (not shown). At 373 K, some of the molecular water desorbs as indicated by the decrease in intensity in OH-stretch and ν_2 bands. The dangling OH band (3695 cm^{-1}) also decreased, and two new bands at ~ 3670 and 3720 cm^{-1} appear as shoulders in the spectrum. By 473 K, the ν_2 band of molecular water is no longer visible, indicating that most or all of the molecular water has desorbed. In addition, the dangling OH band has disappeared, which is also consistent with desorption of the molecular water. Peaks at ~ 3670 and 3720 cm^{-1} are now apparent in the spectrum along with a shoulder at $\sim 3768\text{ cm}^{-1}$. At even higher temperatures, the bands at 3720 and 3768 cm^{-1} persist and a weak band centered at $\sim 3596\text{ cm}^{-1}$ emerges. For $473\text{ K} \leq T \leq 673\text{ K}$, these DRIFTS spectra are similar to IR spectra reported by LaValley et al. (Figure 8f–h).⁴⁹ In that case, four bands at 3785, 3770, 3730, and 3675 cm^{-1} were assigned to surface hydroxyls. For those experiments, the sample preparation was similar to the procedure used here: The α -alumina particles were heated in air at 873 K to remove contaminants and exposed to water vapor at 673 K, and then the samples were evacuated at 473–673 K. (Note that for the experiments of LaValley et al., no molecular water remained on the surface because the samples were

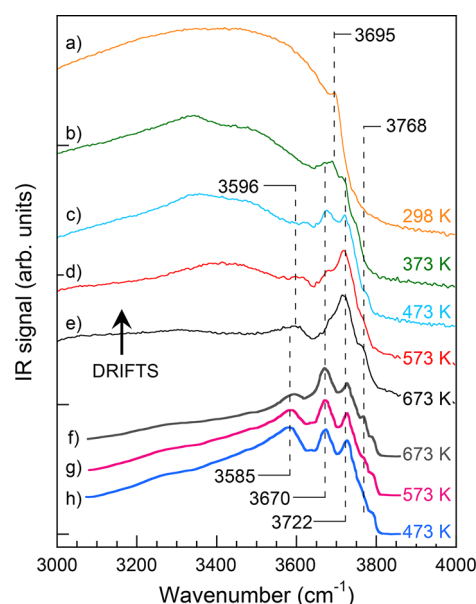


Figure 8. IR spectra of α -alumina particles. (a) DRIFTS for alumina particles with adsorbed water at 298 K. Molecular water adsorbed on the hydroxylated particles obscures the OH-stretch bands of those hydroxyls, but the dangling OH peak of molecular water (3695 cm^{-1}) is seen. (b–e) DRIFTS for the sample shown in (a) heated to temperatures from 373 to 673 K. For $T \geq 473\text{ K}$, all the molecular water has desorbed, and the remaining bands are associated with surface hydroxyls. (f–h) Previously reported IR spectra for hydroxylated α -alumina particles.⁴⁹ Once the molecular water has desorbed (i.e., (c)–(e)), the observed OH-stretch bands match the earlier observations.

pumped out at temperatures where the molecular water desorbed, leaving only the hydroxyls.)

The assignment of the hydroxyls to various configurations on alumina surfaces has been discussed previously.^{2,50,68} For single-coordinated (“terminal”) hydroxyls, Busca has argued that the OH-stretch bands are found at frequencies above 3700 cm^{-1} , while the OH-stretch bands for double- and triple-coordinated hydroxyls occur at frequencies below 3700 cm^{-1} .⁵⁰ For the octahedrally coordinated Al ions in α -alumina, the terminal OH band is at $\sim 3730\text{ cm}^{-1}$.^{50,68} For the α -alumina particles shown in Figure 8, this band is prominent once the molecular water has desorbed, which is consistent with the assignment. However, for the single-crystal experiments, the peak at 3696 cm^{-1} does not correspond to the terminal OH band (see Figure 7) or the other bands seen on the particles and no other bands above 3700 cm^{-1} were found.

Comparison of the DRIFTS (Figure 8) and water TPD results on the α -alumina particles (Figure 1a, purple line) indicates that desorption of molecular water contributes to the TPD peak at $\sim 405\text{ K}$. Because the loss of the molecular water is associated with the reemergence of the surface hydroxyl peaks in the IR spectra, it suggests the water was participating in hydrogen bonds with the hydroxyls. The lack of a similar high-temperature peak for water desorbing from the Al-terminated (0001) surface (see Figure 1a) is consistent with the hypothesis that few if any hydroxyls are present on that surface. The interaction between the adsorbed water and the surface hydroxyls on the alumina particles apparent in the DRIFTS spectra are also relevant to vSFG measurements investigating the interaction of liquid water with $\alpha\text{-Al}_2\text{O}_3$ (0001): Several experiments have observed a relatively

narrow peak at $\sim 3700\text{ cm}^{-1}$ that has been identified with terminal hydroxyls on the surface.^{13,67} Interestingly, the same peak is observed for the air/ $\alpha\text{-Al}_2\text{O}_3(0001)$ interface. It is noteworthy that this peak aligns precisely with the dangling OH peak of air/water interfaces⁶⁹ and seems to be unchanged when water adsorbs on those surfaces.¹³ Braunschweig et al. proposed that the unchanging peak at $\sim 3700\text{ cm}^{-1}$ is associated with OH groups in pores left on the surface by the sample preparation and that, for a surface without these pores, the 3700 cm^{-1} peak was absent at the water/ $\alpha\text{-Al}_2\text{O}_3(0001)$ interface.⁶⁶ The DRIFTS data, which show that the surface hydroxyls interact strongly with adsorbed water, support this latter hypothesis.

The differences in the IR spectra for the α -alumina particles at ambient conditions (Figure 8) and the Al-terminated (0001) surface in UHV (Figures 5 and 6) indicate that there are important differences between these two experiments. The differences could arise for a variety of reasons (e.g., faceted particles versus a single crystal, ambient conditions versus UHV, different sample preparation procedures, etc.). To better understand the origins of these differences, it is instructive to compare the IRAS results presented here to previous experiments on single crystals that were exposed to water vapor at pressures ranging from ~ 0.2 to 20 Torr at 296 K (Figure 9).⁷⁰ For those experiments, a stack of 12 α -

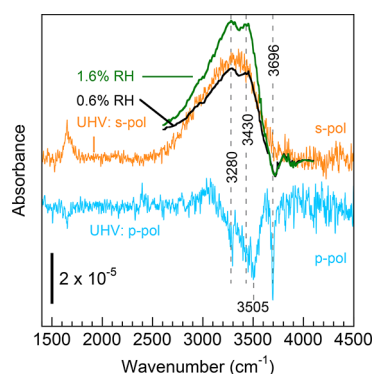


Figure 9. Comparison of IR spectra for water adsorbed on $\alpha\text{-Al}_2\text{O}_3(0001)$ in UHV at $T < 70\text{ K}$ (orange and blue lines for s- and p-polarized light, respectively) and at room temperature and relative humidities (RH) of 0.6 and 1.6% (black and green lines, respectively).⁷⁰ The water coverage for the experiments in UHV was 1 ML. The experiments on the room temperature samples used 12 two-sided (0001) crystals. Therefore, the reported absorbances have been divided by 24. The close correspondence between the spectra in UHV and ambient conditions suggests that the structures of the water adlayers were similar in both conditions.

$\text{Al}_2\text{O}_3(0001)$ single crystals, which were polished on both sides, were prepared by annealing in air at 873 K for several hours. Therefore, the sample preparation was very similar to the one used here for the alumina particles. The single-crystal samples were then exposed to water vapor for approximately 20 min before the absorbance was measured in transmission mode. The samples were tilted at 45° with respect to the IR beam, so the spectra were sensitive to vibrations both parallel and perpendicular to the surface. Because there were 24 surfaces contributing to those experiments, the reported absorbance spectra were divided by 24 to compare to our results obtained in UHV on a single surface. To further facilitate comparison, the s-polarized IRAS absorbance data, which always show negative absorbances on dielectric substrates,^{36,37} have been

inverted. As seen in Figure 9, there is a very close correspondence, in both the magnitude of the absorbance and the shape of the spectra, between the s-polarized spectra for $\theta = 1\text{ ML}$ obtained in UHV (orange line) and the spectra obtained at water vapor pressures of $\sim 0.2\text{ Torr}$ at 300 K. The results indicate that the structures of the water layers formed on these surfaces, which were prepared in two different ways, are the same or very similar. Therefore, the results indicate that dissociative adsorption of water on $\alpha\text{-Al}_2\text{O}_3(0001)$ is a minor channel even after 20 min at much higher vapor pressures. As noted by Al-Abadleh and Grassian, their spectra do show a weak, narrow dip in the signal at $\sim 3710\text{ cm}^{-1}$, which could arise from some dangling hydroxyls on the surface used as the reference.⁷⁰ However, our UHV results suggest that the coverage of these hydroxyls is quite small.

The results in Figure 9 indicate that annealing $\alpha\text{-Al}_2\text{O}_3(0001)$ single crystals in air at $\sim 873\text{ K}$ can produce a (nearly) hydroxyl-free, Al-terminated surface, at least in some cases. Once prepared, the conversion of this surface to a hydroxylated surface is slow.^{5,8,9,20} As noted by Tong et al.,²⁰ various experiments report a wide range of times and/or water vapor pressures required to convert the Al-terminated (0001) surface to the hydroxylated surface,^{5,8,9,20} perhaps arising from the various techniques used for preparing the samples. In contrast, annealing α -alumina particles in air either leaves hydroxyls on the surfaces, or it produces surfaces which readily hydroxylate upon exposure to water (e.g., Figure 8).^{49,68} One possibility is that the hydroxylation reactions are initiated at “defects” on the surface (such as step edges, edges between different facets, vacancies, etc.) and not on the defect-free terraces that were considered in the calculations.¹⁵ Because (1) the fraction of the surface at or near defects is expected to be higher on particles compared to single crystal surfaces and (2) different surface preparation techniques could lead to differences in the defect densities on nominally identical (0001) single crystals, this hypothesis could potentially explain why the reported hydroxylation kinetics have varied so much. Schneider and co-workers investigated possible reaction sequences that involved the sequential addition of OH groups to surface aluminum atoms that would transform a defect-free, Al-terminated (0001) surface to the fully hydroxylated (“gibbsite-like”) surface.¹⁵ Those calculations showed that the intermediate states are higher energy and thus not kinetically favored, i.e., consistent with experimentally observed slow hydroxylation kinetics on single crystals. However, those calculations also predict facile dissociation of water on the exposed aluminum ions during the initial stages of water adsorption, which is not observed in the experiments. We are not aware of any comparable calculations investigating hydroxylation reactions on defective α -alumina surfaces. Collectively, these results point to a lack of a detailed understanding of how hydroxylation proceeds on the surfaces of α -alumina and point out the need for more research on this topic.

IV. CONCLUSIONS

We have investigated the adsorption and reaction of thin water films on single-crystal $\alpha\text{-Al}_2\text{O}_3(0001)$ and α -alumina particles. For alumina particles, the IR spectra indicate that molecular water adsorbs on the hydroxylated surface at room temperature. The molecular water desorbs at $T < 473\text{ K}$, revealing several absorbance bands associated with the surface hydroxyls. For water adsorbed on $\alpha\text{-Al}_2\text{O}_3(0001)$ in UHV, IR spectroscopy

shows that molecular water is present at coverages as low as 1 water molecule per surface aluminum ion but shows no evidence of the surface hydroxyls expected from dissociation. Electron-stimulated desorption indicates molecular water adsorption at even lower coverages. For coverages of 1 ML or less, the water probably adsorbs in two-dimensional islands which have few if any non-hydrogen-bonded ("dangling") OH groups. The water films completely cover the (0001) surface when the coverage reaches ~ 1 ML, and the films grow layer-by-layer for at least the first two layers. Water desorbs from α -Al₂O₃(0001) over a wide temperature range, leaving a hydroxyl-free surface after heating above ~ 800 K. The IR spectra obtained in UHV are quite similar to previously reported spectra for water adsorbed on the (0001) surface at ambient conditions,⁷⁰ which suggests that the (0001) surface prepared by annealing in air at high temperature can also be largely hydroxyl-free. The experimental evidence for the (meta)-stability of molecular water adsorbed on the aluminum-terminated (0001) surface at very low coverages is difficult to reconcile with calculations predicting rapid dissociative adsorption of water on that surface. More research is needed to understand why the experiments and theory indicate such different reactivities for this important surface.

AUTHOR INFORMATION

Corresponding Author

*E-mail: gregory.kimmel@pnnl.gov (G.A.K.).

ORCID

Nikolay G. Petrik: 0000-0001-7129-0752

Greg A. Kimmel: 0000-0003-4447-2440

Notes

The authors declare no competing financial interest.

ACKNOWLEDGMENTS

This work was supported as part of IDREAM (Interfacial Dynamics in Radioactive Environments and Materials), an Energy Frontier Research Center funded by the U.S. Department of Energy, Office of Science, Basic Energy Sciences. Pacific Northwest National Laboratory (PNNL) is a multiprogram national laboratory operated for Department of Energy by Battelle. The experiments on α -Al₂O₃(0001) were performed in the Environmental Molecular Sciences Laboratory, a national scientific user facility sponsored by the Department of Energy's Office of Biological and Environmental Research and located at PNNL. The authors thank Prof. Ian Carmichael for making available the facilities of the Notre Dame Radiation Laboratory, which is supported by DOE BES through Grant DE-FC02-04ER15533.

REFERENCES

- (1) Henrich, V. E.; Cox, P. A. *The Surface Science of Metal Oxides*; Cambridge University Press: Cambridge, 1994.
- (2) Knozinger, H.; Ratnasamy, P. Catalytic Aluminas - Surface Models and Characterization of Surface Sites. *Catal. Rev.: Sci. Eng.* **1978**, *17*, 31–70.
- (3) Robinson, G. N.; Freedman, A.; Kolb, C. E.; Worsnop, D. R. Decomposition of Halomethanes on alpha-Alumina at Stratospheric Temperatures. *Geophys. Res. Lett.* **1994**, *21*, 377–380.
- (4) Dai, Q.; Robinson, G. N.; Freedman, A. Reactions of Halomethanes with Gamma-Alumina Surfaces 1. An Infrared Spectroscopic Study. *J. Phys. Chem. B* **1997**, *101*, 4940–4946.
- (5) Coustet, V.; Jupille, J. High-Resolution Electron-Energy-Loss Spectroscopy of Isolated Hydroxyl-Groups on alpha-Al₂O₃(0001). *Surf. Sci.* **1994**, *307-309*, 1161–1165.
- (6) McHale, J. M.; Auroux, A.; Perrotta, A. J.; Navrotsky, A. Surface Energies and Thermodynamic Phase Stability in Nanocrystalline Aluminas. *Science* **1997**, *277*, 788–791.
- (7) Hass, K. C.; Schneider, W. F.; Curioni, A.; Andreoni, W. The Chemistry of Water on Alumina Surfaces: Reaction Dynamics from First Principles. *Science* **1998**, *282*, 265–268.
- (8) Elam, J. W.; Nelson, C. E.; Cameron, M. A.; Tolbert, M. A.; George, S. M. Adsorption of H₂O on a Single-Crystal alpha-Al₂O₃(0001) Surface. *J. Phys. Chem. B* **1998**, *102*, 7008–7015.
- (9) Liu, P.; Kendelewicz, T.; Brown, G. E.; Nelson, E. J.; Chambers, S. A. Reaction of Water Vapor with alpha-Al₂O₃(0001) and alpha-Fe₂O₃(0001) Surfaces: Synchrotron X-ray Photoemission Studies and Thermodynamic Calculations. *Surf. Sci.* **1998**, *417*, 53–65.
- (10) Eng, P. J.; Trainor, T. P.; Brown, G. E.; Waychunas, G. A.; Newville, M.; Sutton, S. R.; Rivers, M. L. Structure of the Hydrated alpha-Al₂O₃(0001) Surface. *Science* **2000**, *288*, 1029–1033.
- (11) Lodziana, Z.; Norskov, J. K.; Stoltze, P. The Stability of the Hydroxylated (0001) Surface of alpha-Al₂O₃. *J. Chem. Phys.* **2003**, *118*, 11179–11188.
- (12) Deng, X.; Herranz, T.; Weis, C.; Bluhm, H.; Salmeron, M. Adsorption of Water on Cu₂O and Al₂O₃ Thin Films. *J. Phys. Chem. C* **2008**, *112*, 9668–9672.
- (13) Zhang, L.; Tian, C.; Waychunas, G. A.; Shen, Y. R. Structures and Charging of alpha-Alumina (0001)/Water Interfaces Studied by Sum-Frequency Vibrational Spectroscopy. *J. Am. Chem. Soc.* **2008**, *130*, 7686–7694.
- (14) Ranea, V. A.; Schneider, W. F.; Carmichael, I. DFT Characterization of Coverage Dependent Molecular Water Adsorption Modes on alpha-Al₂O₃(0001). *Surf. Sci.* **2008**, *602*, 268–275.
- (15) Ranea, V. A.; Carmichael, I.; Schneider, W. F. DFT Investigation of Intermediate Steps in the Hydrolysis of alpha-Al₂O₃(0001). *J. Phys. Chem. C* **2009**, *113*, 2149–2158.
- (16) Thissen, P.; Grundmeier, G.; Wippermann, S.; Schmidt, W. G. Water Adsorption on the alpha-Al₂O₃(0001) Surface. *Phys. Rev. B: Condens. Matter Mater. Phys.* **2009**, *80*, 245403.
- (17) Wang, B.; Hou, H.; Luo, Y.; Li, Y.; Zhao, Y.; Li, X. Density Functional/All-Electron Basis Set Slab Model Calculations of the Adsorption/Dissociation Mechanisms of Water on alpha-Al₂O₃(0001) Surface. *J. Phys. Chem. C* **2011**, *115*, 13399–13411.
- (18) Argyris, D.; Ho, T. A.; Cole, D. R.; Striolo, A. Molecular Dynamics Studies of Interfacial Water at the Alumina Surface. *J. Phys. Chem. C* **2011**, *115*, 2038–2046.
- (19) Kirsch, H.; Wirth, J.; Tong, Y. J.; Wolf, M.; Saalfank, P.; Campen, R. K. Experimental Characterization of Unimolecular Water Dissociative Adsorption on alpha-Alumina. *J. Phys. Chem. C* **2014**, *118*, 13623–13630.
- (20) Tong, Y. J.; Wirth, J.; Kirsch, H.; Wolf, M.; Saalfank, P.; Campen, R. K. Optically Probing Al-O and O-H Vibrations to Characterize Water Adsorption and Surface Reconstruction on Alpha-Alumina: An Experimental and Theoretical Study. *J. Chem. Phys.* **2015**, *142*, 054704.
- (21) Ma, S. Y.; Liu, L. M.; Wang, S. Q. Water Film Adsorbed on the alpha-Al₂O₃(0001) Surface: Structural Properties and Dynamical Behaviors from First-Principles Molecular Dynamics Simulations. *J. Phys. Chem. C* **2016**, *120*, 5398–5409.
- (22) Tuladhar, A.; Dewan, S.; Kubicki, J. D.; Borguet, E. Spectroscopy and Ultrafast Vibrational Dynamics of Strongly Hydrogen Bonded OH Species at the alpha-Al₂O₃(11(2)over-bar0)/H₂O Interface. *J. Phys. Chem. C* **2016**, *120*, 16153–16161.
- (23) Reiff, S. C.; LaVerne, J. A. Radiolysis of Water with Aluminum Oxide Surfaces. *Radiat. Phys. Chem.* **2017**, *131*, 46–50.
- (24) Ahn, J.; Rabalais, J. W. Composition and Structure of the Al₂O₃{0001}-(1 × 1) Surface. *Surf. Sci.* **1997**, *388*, 121–131.
- (25) Soares, E. A.; Van Hove, M. A.; Walters, C. F.; McCarty, K. F. Structure of the alpha-Al₂O₃(0001) Surface from Low-Energy Electron Diffraction: Al Termination and Evidence for Anomalous Large

Thermal Vibrations. *Phys. Rev. B: Condens. Matter Mater. Phys.* **2002**, *65*, 195405.

(26) Frank, I.; Marx, D.; Parrinello, M. Structure and Electronic Properties of Quinizarin Chemisorbed on Alumina. *J. Chem. Phys.* **1996**, *104*, 8143–8150.

(27) Hass, K. C.; Schneider, W. F.; Curioni, A.; Andreoni, W. First-Principles Molecular Dynamics Simulations of H₂O on α -Al₂O₃(0001). *J. Phys. Chem. B* **2000**, *104*, 5527–5540.

(28) Petrenko, V. F.; Whitworth, R. W. *Physics of Ice*; Oxford University Press: Oxford, 1999; p 373.

(29) Nelson, C. E.; Elam, J. W.; Cameron, M. A.; Tolbert, M. A.; George, S. M. Desorption of H₂O from a Hydroxylated Single-Crystal α -Al₂O₃(0001) Surface. *Surf. Sci.* **1998**, *416*, 341–353.

(30) de Leeuw, N. H.; Parker, S. C. Effect of Chemisorption and Physisorption of Water on the Surface Structure and Stability of α -Alumina. *J. Am. Ceram. Soc.* **1999**, *82*, 3209–3216.

(31) Petrik, N. G.; Henderson, M. A.; Kimmel, G. A. Insights into Acetone Photochemistry on Rutile TiO₂(110). 1. Off-Normal CH₃ Ejection from Acetone Diolate. *J. Phys. Chem. C* **2015**, *119*, 12262–12272.

(32) Kimmel, G. A.; Baer, M.; Petrik, N. G.; VandeVondele, J.; Rousseau, R.; Mundy, C. J. Polarization- and Azimuth-Resolved Infrared Spectroscopy of Water on TiO₂(110): Anisotropy and the Hydrogen-Bonding Network. *J. Phys. Chem. Lett.* **2012**, *3*, 778–784.

(33) Kimmel, G. A.; Petrik, N. G.; Dohnalek, Z.; Kay, B. D. Layer-by-Layer Growth of Thin Amorphous Solid Water Films on Pt(111) and Pd(111). *J. Chem. Phys.* **2006**, *125*, 044713.

(34) Kimmel, G. A.; Petrik, N. G.; Dohnalek, Z.; Kay, B. D. Crystalline Ice Growth on Pt(111): Observation of a Hydrophobic Water Monolayer. *Phys. Rev. Lett.* **2005**, *95*, 166102.

(35) Petrik, N. G.; Kimmel, G. A. Electron-Stimulated Production of Molecular Hydrogen at the Interfaces of Amorphous Solid Water Films on Pt(111). *J. Chem. Phys.* **2004**, *121*, 3736–3744.

(36) Chabal, Y. J. Surface Infrared-Spectroscopy. *Surf. Sci. Rep.* **1988**, *8*, 211–357.

(37) Hansen, W. N. Electric Fields Produced by Propagation of Plane Coherent Electromagnetic Radiation in a Stratified Medium. *J. Opt. Soc. Am.* **1968**, *58*, 380.

(38) Brown, D. E.; George, S. M.; Huang, C.; Wong, E. K. L.; Rider, K. B.; Smith, R. S.; Kay, B. D. H₂O Condensation Coefficient and Refractive Index for Vapor-Deposited Ice from Molecular Beam and Optical Interference Measurements. *J. Phys. Chem.* **1996**, *100*, 4988.

(39) Batista, E. R.; Ayotte, P.; Bilic, A.; Kay, B. D.; Jonsson, H. What Determines the Sticking Probability of Water Molecules on Ice? *Phys. Rev. Lett.* **2005**, *95*, 223201.

(40) Henderson, M. A. The Interaction of Water with Solid Surfaces: Fundamental Aspects Revisited. *Surf. Sci. Rep.* **2002**, *46*, 1.

(41) Petrik, N. G.; Kimmel, G. A. Electron-Stimulated Sputtering of Thin Amorphous Solid Water Films on Pt(111). *J. Chem. Phys.* **2005**, *123*, 054702.

(42) Petrik, N. G.; Kimmel, G. A. Hydrogen Bonding, H-D Exchange, and Molecular Mobility in Thin Water Films on TiO₂(110). *Phys. Rev. Lett.* **2007**, *99*, 196103.

(43) Smith, R. S.; Petrik, N. G.; Kimmel, G. A.; Kay, B. D. Thermal and Nonthermal Physiochemical Processes in Nanoscale Films of Amorphous Solid Water. *Acc. Chem. Res.* **2012**, *45*, 33–42.

(44) Ogasawara, H.; Yoshinobu, J.; Kawai, M. Clustering Behavior of Water (D₂O) on Pt(111). *J. Chem. Phys.* **1999**, *111*, 7003–7009.

(45) Clay, C.; Haq, S.; Hodgson, A. Hydrogen Bonding in Mixed OH + H₂O Overlayers on Pt(111). *Phys. Rev. Lett.* **2004**, *92*, 046102.

(46) Carrasco, J.; Michaelides, A.; Forster, M.; Haq, S.; Raval, R.; Hodgson, A. A One-Dimensional Ice Structure Built from Pentagons. *Nat. Mater.* **2009**, *8*, 427–431.

(47) Kimmel, G. A.; Matthiesen, J.; Baer, M.; Mundy, C. J.; Petrik, N. G.; Smith, R. S.; Dohnalek, Z.; Kay, B. D. No Confinement Needed: Observation of a Metastable Hydrophobic Wetting Two-Layer Ice on Graphene. *J. Am. Chem. Soc.* **2009**, *131*, 12838–12844.

(48) Petrik, N. G.; Kimmel, G. A. Reaction Kinetics of Water Molecules with Oxygen Vacancies on Rutile TiO₂(110). *J. Phys. Chem. C* **2015**, *119*, 23059–23067.

(49) Lavalley, J. C.; Bensitel, M.; Gallas, J. P.; Lamotte, J.; Busca, G.; Lorenzelli, V. FT-IR Study of the Delta-(OH) Mode of Surface Hydroxy-Groups on Metal-Oxides. *J. Mol. Struct.* **1988**, *175*, 453–458.

(50) Busca, G. The Surface of Transitional Aluminas: A Critical Review. *Catal. Today* **2014**, *226*, 2–13.

(51) Bertie, J. E.; Labbe, H. J.; Whalley, E. Absorptivity of Ice I in Range 4000–30 cm⁻¹. *J. Chem. Phys.* **1969**, *50*, 4501.

(52) Cholette, F.; Zubkov, T.; Smith, R. S.; Dohnalek, Z.; Kay, B. D.; Ayotte, P. Infrared Spectroscopy and Optical Constants of Porous Amorphous Solid Water. *J. Phys. Chem. B* **2009**, *113*, 4131–4140.

(53) Libowitzky, E. Correlation of O-H Stretching Frequencies and O-H...O Hydrogen Bond Lengths in Minerals. *Monatsh. Chem.* **1999**, *130*, 1047–1059.

(54) Feibelman, P. J.; Kimmel, G. A.; Smith, R. S.; Petrik, N. G.; Zubkov, T.; Kay, B. D. A Unique Vibrational Signature of Rotated Water Monolayers on Pt(111): Predicted and Observed. *J. Chem. Phys.* **2011**, *134*, 204702.

(55) Biswas, R.; Carpenter, W.; Fournier, J. A.; Voth, G. A.; Tokmakoff, A. IR Spectral Assignments for the Hydrated Excess Proton in Liquid Water. *J. Chem. Phys.* **2017**, *146*, 154507.

(56) Thamer, M.; De Marco, L.; Ramasesha, K.; Mandal, A.; Tokmakoff, A. Ultrafast 2D IR Spectroscopy of the Excess Proton in Liquid Water. *Science* **2015**, *350*, 78–82.

(57) Rowland, B.; Devlin, J. P. Spectra of Dangling OH Groups at Ice Cluster Surfaces and within Pores of Amorphous Ice. *J. Chem. Phys.* **1991**, *94*, 812.

(58) Zubkov, T.; Smith, R. S.; Engstrom, T. R.; Kay, B. D. Adsorption, Desorption, and Diffusion of Nitrogen in a Model Nanoporous Material. I. Surface Limited Desorption Kinetics in Amorphous Solid Water. *J. Chem. Phys.* **2007**, *127*, 184707.

(59) On reduced TiO₂(110), water dissociatively adsorbs in vacancies on the surface, creating two bridging hydroxyls for each vacancy until all the vacancies are filled. The surface where all the vacancies have been replaced with twice as many bridging hydroxyls is called hydroxylated-TiO₂(110), or h-TiO₂(110).

(60) Daschbach, J. L.; Peden, B. M.; Smith, R. S.; Kay, B. D. Adsorption, Desorption, and Clustering of H₂O on Pt(111). *J. Chem. Phys.* **2004**, *120*, 1516–1523.

(61) Rosu-Finsen, A.; Marchione, D.; Salter, T. L.; Stubbing, J. W.; Brown, W. A.; McCoustra, M. R. Peeling the Astronomical Onion. *Phys. Chem. Chem. Phys.* **2016**, *18*, 31930–31935.

(62) Michaelides, A.; Alavi, A.; King, D. A. Insight into H₂O-Ice Adsorption and Dissociation on Metal Surfaces from First-Principles Simulations. *Phys. Rev. B: Condens. Matter Mater. Phys.* **2004**, *69*, 113404.

(63) Kimmel, G. A.; Zubkov, T.; Smith, R. S.; Petrik, N. G.; Kay, B. D. Turning Things Downside Up: Adsorbate Induced Water Flipping on Pt(111). *J. Chem. Phys.* **2014**, *141*, 18c515.

(64) Kelber, J. A.; Niu, C. Y.; Shepherd, K.; Jennison, D. R.; Bogicevic, A. Copper Wetting of α -Al₂O₃(0001): Theory and Experiment. *Surf. Sci.* **2000**, *446*, 76–88.

(65) Niu, C.; Shepherd, K.; Martini, D.; Tong, J.; Kelber, J. A.; Jennison, D. R.; Bogicevic, A. Cu Interactions with α -Al₂O₃(0001): Effects of Surface Hydroxyl Groups Versus Dehydroxylation by Ar-Ion Sputtering. *Surf. Sci.* **2000**, *465*, 163–176.

(66) Braunschweig, B.; Eissner, S.; Daum, W. Molecular Structure of a Mineral/Water Interface: Effects of Surface Nanoroughness of α -Al₂O₃(0001). *J. Phys. Chem. C* **2008**, *112*, 1751–1754.

(67) Florsheimer, M.; Kruse, K.; Polly, R.; Abdelmonem, A.; Schimmelpfennig, B.; Klenze, R.; Fanghanel, T. Hydration of Mineral Surfaces Probed at the Molecular Level. *Langmuir* **2008**, *24*, 13434–13439.

(68) Busca, G.; Lorenzelli, V.; Ramis, G.; Willey, R. J. Surface Sites on Spinel-Type and Corundum-Type Metal-Oxide Powders. *Langmuir* **1993**, *9*, 1492–1499.

(69) Du, Q.; Superfine, R.; Freysz, E.; Shen, Y. R. Vibrational Spectroscopy of Water at the Vapor Water Interface. *Phys. Rev. Lett.* **1993**, *70*, 2313–2316.

(70) Al-Abadleh, H. A.; Grassian, V. H. FT-IR Study of Water Adsorption on Aluminum Oxide Surfaces. *Langmuir* **2003**, *19*, 341–347.